

NANO EXPRESS

Open Access

Three strategies to stabilise nearly monodispersed silver nanoparticles in aqueous solution

Amadeus PZ Stevenson¹, Duani Blanco Bea², Sergi Civit³, Sonia Antoranz Contera^{1,4}, Alberto Iglesias Cerveto² and Sonia Trigueros^{1,4*}

Abstract

Silver nanoparticles are extensively used due to their chemical and physical properties and promising applications in areas such as medicine and electronics. Controlled synthesis of silver nanoparticles remains a major challenge due to the difficulty in producing long-term stable particles of the same size and shape in aqueous solution. To address this problem, we examine three strategies to stabilise aqueous solutions of 15 nm citrate-reduced silver nanoparticles using organic polymeric capping, bimetallic core-shell and bimetallic alloying. Our results show that these strategies drastically improve nanoparticle stability by distinct mechanisms. Additionally, we report a new role of polymer functionalisation in preventing further uncontrolled nanoparticle growth. For bimetallic nanoparticles, we attribute the presence of a higher valence metal on the surface of the nanoparticle as one of the key factors for improving their long-term stability. Stable silver-based nanoparticles, free of organic solvents, will have great potential for accelerating further environmental and nanotoxicity studies.

PACS: 81.07.-b; 81.16.Be; 82.70.Dd.

Keywords: silver nanoparticles, stability, functionalisation, monodispersed, aging, toxicity.

Background

Metal nanoparticles have generated great interest for applications in physics, materials, chemistry and biomedical sciences in plasmonics [1], biosensing [2-4], nanomedicine [5-7], nanoelectronics [8], catalysis [9,10], magnetic fluids [11] and dye-based solar cells [12] due to their chemical, electronic, optical and magnetic properties. These applications depend on the availability of homogeneous nanoparticles of controlled size and shape, which remain stable in their complex target environments [13,14]. For example, metal nanoparticles exhibit surface plasmon resonance in the visible spectrum range, resulting in light scattering and characteristic absorbance peaks whose location and width depend on the type of metal, size and shape of the nanostructure and the medium they are immersed in [15-19]. Interactions between nanoparticles and biological matter

will also depend on their size, shape and surface charge as they interact with different organisms [20].

Silver and gold nanoparticles have attracted great interest for many applications due to their strong plasmonic properties and to the availability of methods for synthesis [21,22]. The colloidal method has been extensively used due to the ability to synthesise nanoparticles directly in aqueous solution [23]. However, controlling the size and shape of metal nanoparticles remains challenging; nanoparticles are often heterogeneous in size and shape unless multiple reaction parameters are carefully regulated [22,24]. Synthesis via multiple steps, seed-mediated growth or via organic solvents has overcome several of these problems, although these synthesis methods increase in complexity with the number of steps involved and will limit potential biomedical applications when organic solvents are used [25-27].

The long-term stability of nanoparticles critically depends on the medium they are immersed in. The liquid influences interparticle forces and chemical reactivity, which affect aggregation, size and shape of the

* Correspondence: s.trigueros1@physics.ox.ac.uk

¹Department of Physics, University of Oxford, Parks Road, Oxford, OX1 3PU, UK

Full list of author information is available at the end of the article

nanoparticles and long-term stability ('aging'), especially if the nanoparticles are applied or stored in aqueous conditions [28]. These effects are particularly relevant to more reactive metals such as silver. Stable silver nanoparticles in solution are necessary to apply and assess their interactions with biological matter and living cells. It is difficult to determine the effect of silver nanoparticle solutions where variable sizes, aggregates, surfactants and especially free silver ions are present [29].

A critical step to control the stability of inorganic nanoparticles lies in their surface modification and functionalisation [30,31]. Here, we compare three strategies to functionalise nearly monodispersed silver-based nanoparticles directly in aqueous solution. We have synthesised silver nanoparticles with a narrow shape and size distribution (15 nm quasi-spherical nanoparticles), functionalising them with polyethylene glycol (PEG) [32-34], gold (core-shell) and chromium (alloy). We have characterised the different silver-based nanostructures and established their stability by UV-Visible (UV-Vis) spectroscopy, transmission electron microscopy (TEM) and amplitude modulation atomic force microscopy (AFM) in liquid. We have tested the validity of our results using statistical bootstrapping tools, demonstrating a close relationship between homogeneity of nanoparticle size, shape and particle sphericity. Finally, this study has made it possible to produce stable silver-based nanoparticles that can be used for further applications and studies of toxicity and environmental impact, where the effect of the nanoparticle-containing solution can be attributed to nanoparticles of a controlled size and stability and not to by-products of synthesis (free ions, toxic surfactants), aggregation and/or degradation due to aging effects.

Materials and methods

Unless otherwise stated, all reagents were purchased from Sigma-Aldrich (Dorset, UK), of analytical grade, and were used as received. Milli-Q water (Millipore Co., Billerica, MA, USA; specific resistivity of 18 M Ω cm) was used for the preparation of all solutions. Glassware was cleaned with Milli-Q water prior to the synthesis processes. Muscovite mica was purchased from SPI Supplies (West Chester, PA, USA).

Nanoparticle synthesis

Silver (Ag) nanoparticles capped with citrate were obtained using the Turkevich method [35]. A solution of silver nitrate (125 ml, 1 mM) was heated to 95°C, and a solution of trisodium citrate (7.75 mM) was added. Nearly 15 min later, a colour change was observed indicating the formation of nanoparticles, and the solution was cooled to room temperature and stored at 5°C. During synthesis, we maintained a constant pH of 6.5.

PEG-functionalised silver nanoparticles (AgPEG) were obtained via direct PEGylation [32] by immediately adding a solution of PEG-6000 (80 mM) to freshly synthesised (as mentioned) silver nanoparticles (50 ml). The sample was cooled to -5°C for 8 h before storing at 5°C.

Silver-gold (Ag-Au) nanoshells were obtained by the successive reduction of two metal salts. A fresh solution of silver nanoparticles was prepared as previously described, then immediately heated to 90°C, and a solution of hydrogen tetrachloroaurate (1.2 mM) was added. The reaction mixture was then heated to 95°C, and at this point, a solution of trisodium citrate (7.75 mM) was added. When a colour change was observed, the mixture was cooled gradually to room temperature and stored at 5°C. During the second reaction, chloride ions produced from the reduction of hydrogen tetrachloroaurate reacted with unbound silver forming a silver halide which sedimented rapidly and was removed from the product.

Silver-chromium (AgCr) alloy nanoparticles were synthesised by co-reducing two metal salts. A solution of potassium dichromate dissolved in sulphuric acid (5 ml, 42 mM) was diluted twice in water (10 ml) and added to a solution of silver nitrate (125 ml, 1 mM) before heating to 95°C. A solution of trisodium citrate (7.75 mM) was then added. When a colour change was observed, the mixture was cooled to room temperature and stored at 5°C.

Nanoparticle characterisation

UV-Vis absorption spectra of nanoparticle aqueous solutions were obtained using an MDR-23 monochromator (LOMO, St. Petersburg, Russia). TEM images were obtained using a Tecnai 12 TEM (FEI Company, Eindhoven, The Netherlands) and recorded with a Gatan US1000 2 K CCD camera (Gatan, Inc., Pleasanton, CA, USA). All samples were deposited on formvar-coated 200 mesh copper grids, and the excess liquid wicked off with filter paper. The samples were air-dried and examined unstained. TEM images were analysed in ImageJ 1.43 u (NIH, Bethesda, MD, USA). The area and perimeter of each nanoparticle was extracted before calculating circularity $\left(4\pi \left(\frac{\text{Area}}{\text{Perimeter}^2}\right)\right)$ and diameter $\left(2\sqrt{\frac{\text{Area}}{\pi}}\right)$, estimating particles to be spherical. Both metrics were sensitive to pixel density, with smaller particles yielding larger rounding errors due to the lower number of pixels available.

For atomic force microscopy imaging in liquid (Ag, AgCr), nanoparticle samples (2 μ l) were diluted in NaCl buffer (48 μ l, 20 mM with 50 mM HEPES, pH 6.5) and bath sonicated (Ultrawave U300, Ultrawave, Cardiff, UK)

for 15 min. Samples were incubated on freshly cleaved mica for 20 min at room temperature before imaging in NaCl buffer. Due to PEG hydration, the height of AgPEG nanoparticles characterised by AFM in liquid (data not shown) was found to be twice the value of the diameter from TEM. Consequently, AgPEG nanoparticles were characterised in air by adding 2 μ l of nanoparticle sample onto freshly cleaved mica and air-dried before imaging. Ag-Au nanoparticles were imaged in air after an incubation time of 2 h on freshly cleaved mica coated with poly-L-lysine (0.01%). Samples were imaged with a commercial MFP-3D AFM (Asylum Research, Santa Barbara, CA, USA) operating in amplitude modulation mode. Olympus AC240 ($k = 2 \text{ N m}^{-1}$) silicon cantilever tips in air and Olympus TR800/400 ($k = 0.57 \text{ N m}^{-1}/0.08 \text{ N m}^{-1}$) (all from Olympus Europa Holding GmbH, Hamburg, Germany) silicon nitride cantilevers in liquid were used. Low scan rates (0.3 Hz) further minimised tip sample forces from displacing deposited nanoparticles. Post-scan processing included image flattening and particle size analysis using the manufacturer's provided software (MFP-3D 080501 + 1429), based in Igor Pro 6.04 (WaveMetrics, Inc., Portland, OR, USA). Nanoparticle heights were calculated by thresholding height in topography images and extracting the z range of each particle.

To quantify the relationship between homogeneity of nanoparticle size, shape and aspect ratio, TEM diameters and AFM heights of nanoparticles were combined and described according to the eccentricity statistic distribution ε (Equation 1) via non-parametric bootstrapping:

$$\varepsilon = \sqrt{\frac{a^2 - b^2}{a^2}} = \sqrt{1 - \left(\frac{b}{a}\right)^2} \quad 0 < \varepsilon < 1, \quad (1)$$

where a and b are half of the ellipse's major and minor axes (diameter and height), respectively. As the eccentricity value ranges from 0 to 1, the corresponding nanoparticle shape will range from spherical ($\varepsilon = 0$) to ellipsoidal ($\varepsilon = 1$). The sphericity of nanoparticles that resulted from different stabilisation strategies were then compared using the Kruskal-Wallis hypothesis test [extensive details are provided in Additional file 1].

Results and discussion

Silver nanoparticles functionalised with PEG: organic stability

The synthesised citrate-capped silver nanoparticles were characterised by UV-Vis spectroscopy, TEM and AFM (Figure 1). The UV-Vis spectrum of the nanoparticles exhibited a narrow absorption peak at 433 nm due to plasmon resonance (Figure 1A), indicating a narrow size

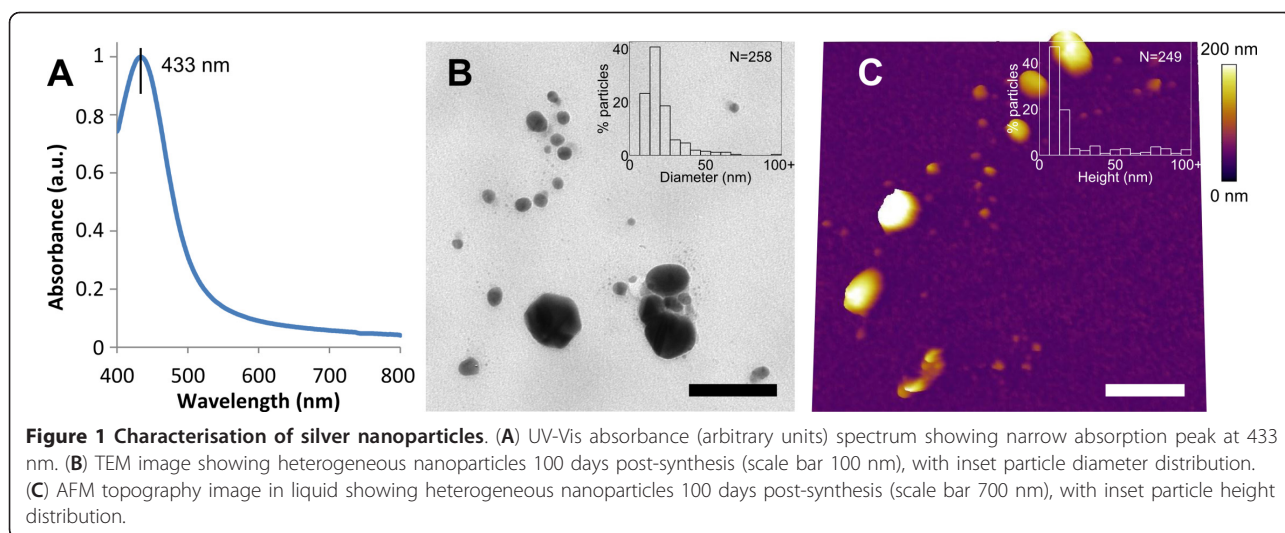
and shape distribution immediately post-synthesis [36]. TEM and AFM data obtained 100 days after synthesis gave a median particle diameter and height of about 14 nm (Figure 1B) and 10 nm (Figure 1C), respectively. Both TEM and AFM data show strong heterogeneity in the size and shape of synthesised nanoparticles. Large ($> 100 \text{ nm}$ in height) aggregates were observed directly in liquid (Figure 1C), confirming that the instability of the observed silver nanoparticles was not due to drying-induced aggregation during TEM sample preparation.

Immediately after synthesis, we functionalised the nanoparticles with PEG via direct PEGylation, a common method to improve their stability [32]. The characterisation of the resulting AgPEG nanoparticles is shown in Figure 2. The UV-Vis spectrum shows a distinct red-shift in the absorbance from 433 to 894 nm (Figure 2A). TEM characterisation gave a median metallic particle diameter of about 47 nm (Figure 2B). AFM characterisation gave a median particle height of about 40 nm (Figure 2C). The observed substantial absorbance shift has been reported during photo-induced conversion of nanospheres to nanoplates [16,37], although we found no evidence of nanoplates during both TEM and AFM characterisations. We speculate that this shift may be due to a complex coupled absorbance phenomenon due to the proximity of the nanoparticles linked with PEG. Drying the sample for AFM in the presence of ethanol, we indeed observed smaller seed particles adsorbed by PEG surrounding the core silver nanoparticles (Figure 2C inset). Trapping seeds in this way will prevent further uncontrolled growth via ripening. The use of PEG as a functionalising agent is common, and its effect is attributed to steric repulsion between PEG chains adsorbed on nanoparticle surfaces [33,34]. We propose that it is the combination of steric repulsion and trapping of seeds that prevents further uncontrolled growth and improves stability. The larger particle size after functionalisation could be explained by the reported activity of PEG as a reducing agent of silver ions [33,38]. PEG may continue to catalyse ion reduction in the nanoparticle solution, consequently increasing nanoparticle size.

To explore the effects of non-steric stabilisations, we functionalised citrate-capped silver nanoparticles with gold to create bimetallic silver-gold nanoshells. Gold nanoparticles synthesised by the Turkevich method are known for their homogeneity [39], which suggests an increased stability between gold and citrate compared with silver and citrate.

Silver-gold nanoshells: bimetallic stability I

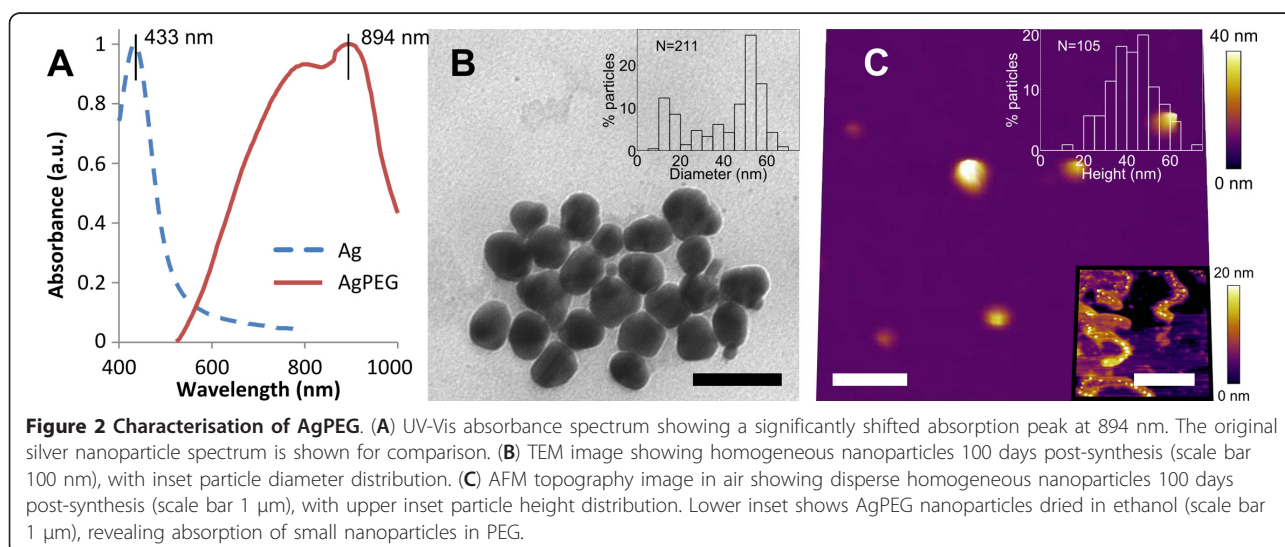
Two types of bimetallic nanoparticles can be obtained: (1) nanoparticles consisting of two metals with well-

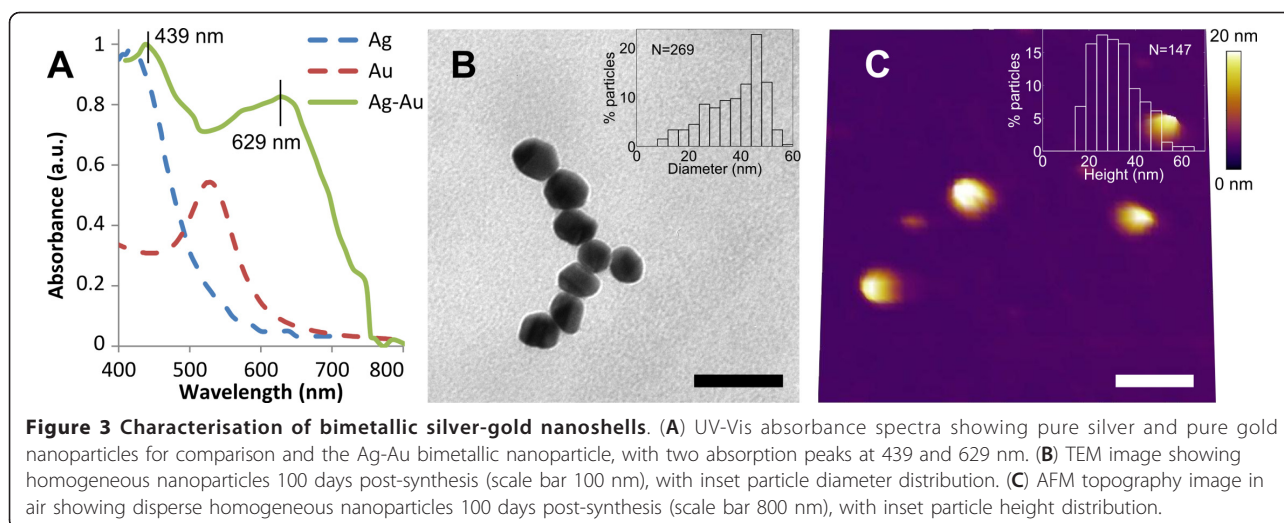


separated distributions called core-shell nanoparticles (nanoshells) and (2) nanoparticles with a homogeneous distribution of two metals called alloys [40]. Nanoshells can be obtained by successive reduction of two metals, where the first metal is reduced to form the core, and the second metal is reduced to form the shell [22]. Figure 3 shows the characterisation of the Ag-Au nanoshells obtained in this work. The UV-Vis spectrum shows two absorption peaks at 439 and 629 nm (Figure 3A). We observe a redshift in the gold peak from 526 to 629 nm and a smaller redshift in the silver peak from 410 to 439 nm. TEM and AFM data obtained 100 days post-synthesis gave a median particle diameter of about 39 nm (Figure 3B) and a median particle height of about 28 nm (Figure 3C), respectively. The small redshift in the silver absorbance peak is most likely due to an increased size of the core during the formation of

the gold shell [17]. An increasing redshift in the gold absorption peak has been reported both experimentally and theoretically with an increasing gold shell thickness, although the chemical composition, dielectric environment and shape of the nanoshells will also affect the position of the absorbance peak [21,41-44]. Due to the sedimentation step during synthesis (see the 'Materials and methods' section), smaller seed-like particles were not observed. The obtained nanoshells were homogeneous in both size and shape, in contrast to the pure silver nanoparticles. The higher valence of gold used (+3 compared with +1 for silver) may affect metal-citrate bonding, with more citrate ions able to bind to each metal ion at the surface, leading to increased stability.

To investigate whether a weak silver-citrate affinity at the nanoparticle surface is responsible for nanoparticle instability, we synthesised silver-chromium alloy





nanoparticles through co-reduction, where chromium also has a higher valence (+3).

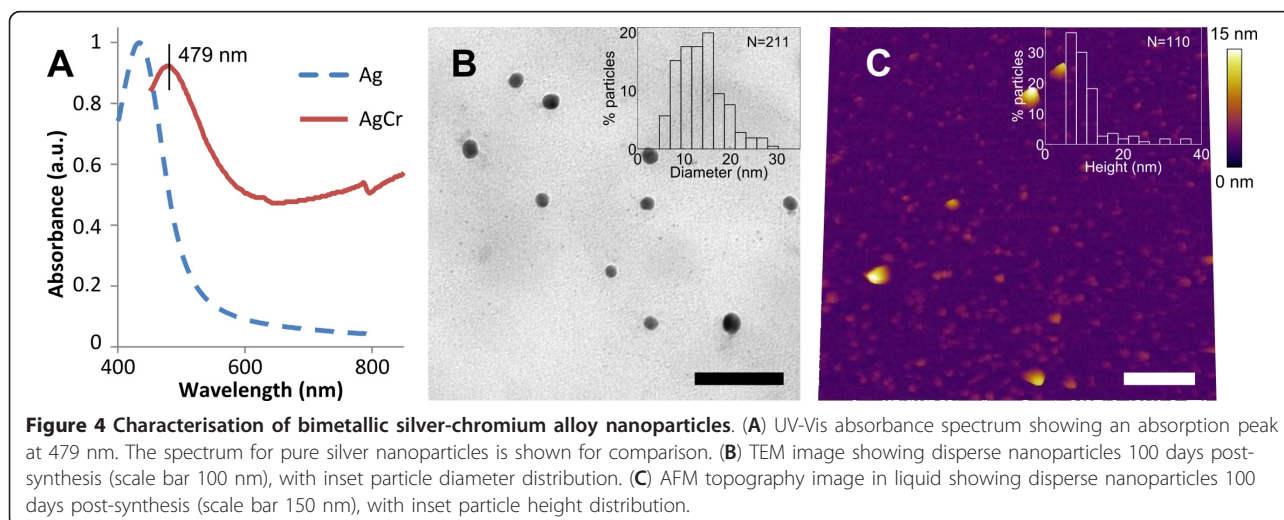
Silver-chromium alloy nanoparticles: bimetallic stability II

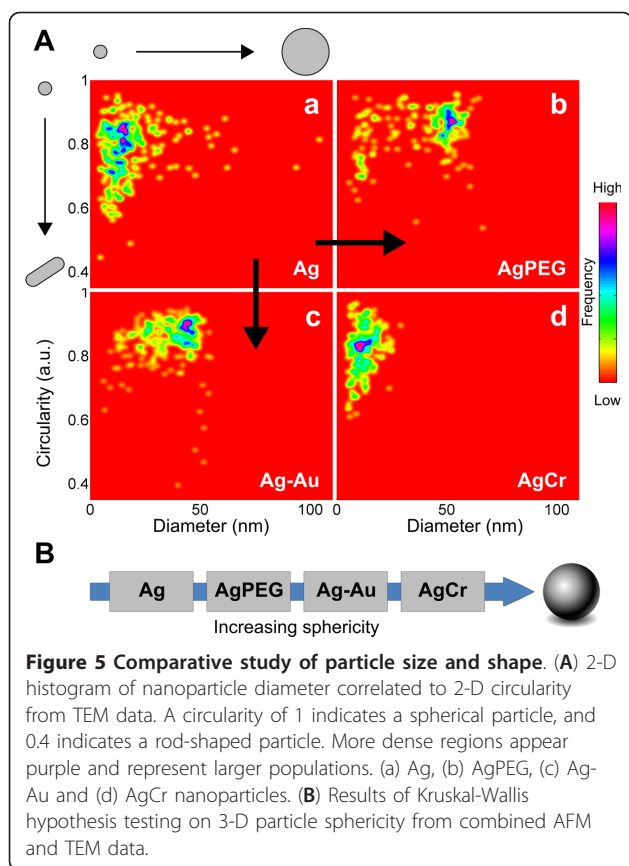
The characterisation of obtained AgCr alloy nanoparticles is shown in Figure 4. The UV-Vis spectrum shows a redshift in the plasmon resonance absorption peak from 433 to 479 nm and a broadening of the spectrum (Figure 4A). TEM and AFM characterisations 100 days post-synthesis gave a median particle diameter of about 12 nm (Figure 4B) and a median particle height of about 7 nm (Figure 4C), respectively. The broadening of the plasmon absorption peak corresponds to the low but broad absorption of Cr^{3+} , and the redshift in the peak is likely due to a combination of the altered composition and dielectric function of the alloy [44,45]. The diameter and height distributions were well confined below 40 nm; however, smaller seeds were numerous.

Despite the presence of these seeds, the alloy nanoparticles remained stable in size, shape and dispersibility confirming that the presence of a higher valence metal (chromium) on the nanoparticle surface significantly improves stability, without requiring the complete capping of the core metal.

Improved stability in shapes and sizes of nanoparticles

To quantify the effects previously described on the size and shape of the obtained nanoparticles, we analysed the TEM data before combining and analysing TEM and AFM data. First, we analysed the TEM nanoparticle profiles. Figure 5 shows two-dimensional (2-D) histograms of nanoparticle diameters and circularities calculated for the nanoparticles that are synthesised in this study. In a TEM image, circularity is defined as the ratio of the area of a nanoparticle with its perimeter, determined via segmentation (see the 'Materials and methods'





section). Circularity ranges from a value of 1 for a circular object (spherical or disc-shaped nanoparticle, with the latter eliminated due to the absence of observed discs) to 0 for a highly elongated object (rod-shaped nanoparticle). In our work, we did not observe any single nanoparticle with a circularity lower than 0.4. Silver nanoparticles ((a) of Figure 5A) were the most heterogeneous in size and shape. Functionalising silver nanoparticles with PEG ((b) of Figure 5A) resulted in particles with an increased diameter and circularity, which are both more narrowly distributed, indicating the predominance of a single species of nanoparticle. AgPEG nanoparticles around 15 nm in diameter observed in the histogram probably remain unfunctionalised. Capping with gold to create the Ag-Au nanoshells ((c) of Figure 5A) resulted in particles with an increased and more narrowly distributed diameter and circularity, again indicating the tendency towards a single species. A small presence of rods was observed, which was expected in the gold functionalisation step as by-products of pure gold rod formation. Finally, AgCr alloy nanoparticles ((d) of Figure 5A) were the most narrowly distributed in size, with no particle diameters above 40 nm. We predominantly observed circular objects although the circularity metric is compromised as particle diameters become

smaller (see the ‘Materials and methods’ section for more details); this explains the broad range of obtained circularities in the case of the smaller AgCr nanoparticles.

Second, we combined TEM diameters with AFM heights to ascertain particle sphericities in three dimensions, where a higher particle sphericity indicates a more stable, homogenous growth process. We found (Figure 5B, with details in Additional file 1) that the nanoparticle sphericities increased with each stabilisation strategy, i.e. unfunctionalised nanoparticles were the least stable, followed by PEG-functionalised, silver-gold nanoshells and silver-chromium alloy nanoparticles.

Conclusions

Due to the highly reactive nature of silver ions and the multiple roles that citrate plays during synthesis, it has been difficult to control the size and shape of citrate-reduced silver nanoparticles without further functionalisation. In this work, we synthesise a 15 nm quasi-spherical silver nanoparticle directly in water without organic solvents. After 100 days in solution, the nanoparticles exhibited increased heterogeneity due to their inherent instability. We used PEG as an organic capping agent and gold as an inorganic capping agent. In both cases, we are effectively able to control further growth and stabilisation of the nanoparticles. We found that the addition of PEG not only stabilises the nanoparticles by steric repulsion and trapping of seeds, but also allows controlled further growth of nanoparticles, improving homogeneity in nanoparticle size, shape and stability. In the case of Ag-Au nanoshells, the higher electron affinity of gold may lead to a stronger gold-citrate interaction at the nanoparticle surface compared with that in the citrate-capped silver nanoparticles, consequently improving size and shape homogeneity and long-term stability. Similarly to gold, the higher valence of chromium may lead to a stronger chromium-citrate interaction at the nanoparticle surface. The alloying process enables the production of stable silver-based nanoparticles without the need for additional functionalisation/capping.

The findings of this work enable further fundamental research on the effects of material, size and shape on nanoparticle behaviour. The ability to understand and control the nanoparticle/liquid interface allows the possibility of studying the role of nanoparticles in further applications where electrolytes are an important consideration for e.g. water treatment and biomedical use (due to the presence of salts in physiological solutions), which is particularly timely for quantitative toxicity studies, given the current and future widespread production and application of silver nanostructures.

Additional material

Additional file 1: Supplementary data. Bootstrap statistical analysis of AFM/TEM data, including non-parametric Kruskal-Wallis hypothesis testing.

Acknowledgements

This project was funded through the Oxford Martin School. ST was supported by the Oxford Martin School. APZS was supported by the EPSRC Life Sciences Interface Doctoral Training Centre. SC was supported by the grant BFU2009-06974 from the Ministry of Science and Innovation of Spain. SAC was supported by RCUK. DBB and AIC were supported by CNIC, Cuba. We thank Dr. Mike Shaw of Sir William Dunn School of Pathology, Oxford for the help in acquiring TEM data. We further thank Dr. Kislon Voitchovsky of EPFL, Switzerland for his invaluable comments on the manuscript.

Author details

¹Department of Physics, University of Oxford, Parks Road, Oxford, OX1 3PU, UK ²Department of Materials, National Centre for Scientific Research, PO Box 6414, Avenida 25 and 158, Cubanacán, Playa, Havana, CP 12100, Cuba ³Department of Statistics, University of Barcelona, Avenida Diagonal 645, Barcelona, 08028, Spain ⁴Institute of Nanoscience for Medicine, Oxford Martin School, 34 Broad Street, University of Oxford, Oxford, OX1 3BD, UK

Authors' contributions

DBB, AIC and ST carried out nanoparticle synthesis, functionalisation and UV-Vis characterisation. APZS carried out the AFM characterisation and AFM/TEM analysis of nanoparticles. SAC helped with AFM characterisation and conceptual discussions. SC constructed and performed the statistical analysis of nanoparticle sphericity. APZS and ST co-wrote the manuscript. ST conceived the study. All authors read and approved the final manuscript.

Competing interests

The authors declare that they have no competing interests.

Received: 22 August 2011 Accepted: 22 February 2012

Published: 22 February 2012

References

- Eichelbaum M, Rademann K: Plasmonic enhancement or energy transfer? On the luminescence of gold-, silver-, and lanthanide-doped silicate glasses and its potential for light-emitting devices. *Adv Funct Mater* 2009, **19**:2045-2052.
- Katz E, Willner I, Wang J: Electroanalytical and bioelectroanalytical systems based on metal and semiconductor nanoparticles. *Electroanalysis* 2004, **16**:19-44.
- Haes AJ, Zou S, Schatz GC, Van Duyne RP: A nanoscale optical biosensor: the long range distance dependence of the localized surface plasmon resonance of noble metal nanoparticles. *J Phys Chem B* 2004, **108**:109-116.
- McFarland AD, Van Duyne RP: Single silver nanoparticles as real-time optical sensors with zeptomole sensitivity. *Nano Lett* 2003, **3**:1057-1062.
- Arvizo R, Bhattacharya R, Mukherjee P: Gold nanoparticles: opportunities and challenges in nanomedicine. *Expert Opin Drug Delivery* 2010, **7**:753-763.
- Cai W, Gao T, Hong H, Sun J: Applications of gold nanoparticles in cancer nanotechnology. *Nanotechnol Sci Appl* 2008, **1**:17-32.
- Cherukuria P, Glazera ES, Curley SA: Targeted hyperthermia using metal nanoparticles. *Adv Drug Delivery Rev* 2010, **62**:339-345.
- Cui Y, Björk MT, Liddle JA, Sönnichsen C, Boussert B, Alivisatos AP: Integration of colloidal nanocrystals into lithographically patterned devices. *Nano Lett* 2004, **4**:1093-1098.
- Chan K-Y, Ding J, Ren J, Cheng S, Tsang KY: Supported mixed metal nanoparticles as electrocatalysts in low temperature fuel cells. *J Mater Chem* 2004, **14**:505-516.
- Vajda S, Pellin MJ, Greeley JP, Marshall CL, Curtiss LA, Ballentine GA, Elam JW, Catillon-Mucherie S, Redfern PC, Mehmood F, Zapol P: Subnanometre platinum clusters as highly active and selective catalysts for the oxidative dehydrogenation of propane. *Nat Mater* 2009, **8**:213-216.
- Gupta AK, Gupta M: Synthesis and surface engineering of iron oxide nanoparticles for biomedical applications. *Biomaterials* 2005, **26**:3995-4021.
- Brown MD, Suteewong T, Kumar RSS, D'Innocenzo V, Petrozza A, Lee MM, Wiesner U, Snaith HJ: Plasmonic dye-sensitized solar cells using core-shell metal-insulator nanoparticles. *Nano Lett* 2011, **11**:438-445.
- Cho EC, Au L, Zhang Q, Xia Y: The effects of size, shape, and surface functional group of gold nanostructures on their adsorption and internalization by cells. *Small* 2010, **6**:517-522.
- El Badawy AM, Luxton TP, Silva RG, Scheckel KG, Suidan MT, Tolaymat TM: Impact of environmental conditions (pH, ionic strength, and electrolyte type) on the surface charge and aggregation of silver nanoparticles suspensions. *Environ Sci Technol* 2010, **44**:1260-1266.
- Creighton JA, Eadon DG: Ultraviolet-visible absorption spectra of the colloidal metallic elements. *J Chem Soc, Faraday Trans* 1991, **87**:3881-3891.
- Jin R, Cao YW, Mirkin CA, Kelly KL, Schatz GC, Zheng JG: Photoinduced conversion of silver nanospheres to nanoprisms. *Science* 2001, **294**:1901-1903.
- Stamplecoksie KG, Scaiano JC, Tiwari VS, Anis H: Optimal size of silver nanoparticles for surface-enhanced Raman spectroscopy. *J Phys Chem C* 2011, **115**:1403-1409.
- Mock JJ, Barbic M, Smith DR, Schultz DA, Schultz S: Shape effects in plasmon resonance of individual colloidal silver nanoparticles. *J Chem Phys* 2002, **116**:6755-6759.
- Kelly KL, Coronado E, Zhao LL, Schatz GC: The optical properties of metal nanoparticles: the influence of size, shape, and dielectric environment. *J Phys Chem B* 2003, **107**:668-677.
- Verma A, Stellacci F: Effect of surface properties on nanoparticle-cell interactions. *Small* 2010, **6**:12-21.
- Mulvaney P: Surface plasmon spectroscopy of nanosized metal particles. *Langmuir* 1996, **12**:788-800.
- Zhang Q, Xie J, Yu Y, Lee JY: Monodispersity control in the synthesis of monometallic and bimetallic quasi-spherical gold and silver nanoparticles. *Nanoscale* 2010, **2**:1962-1975.
- Yin Y, Alivisatos AP: Colloidal nanocrystal synthesis and the organic-inorganic interface. *Nature* 2005, **437**:664-670.
- Chen B, Jiao X, Chen D: Size-controlled and size-designed synthesis of nano/submicrometer Ag particles. *Cryst Growth Des* 2010, **10**:3378-3386.
- Jana NR, Gearheart L, Murphy CJ: Seeding growth for size control of 5-40 nm diameter gold nanoparticles. *Langmuir* 2001, **17**:6782-6786.
- Dong X, Ji X, Wu H, Zhao L, Li J, Yang W: Shape control of silver nanoparticles by stepwise citrate reduction. *J Phys Chem C* 2009, **113**:6573-6576.
- Jana NR, Peng X: Single-phase and gram-scale routes toward nearly monodisperse Au and other noble metal nanocrystals. *J Am Chem Soc* 2003, **125**:14280-14281.
- Min Y, Akbulut M, Kristiansen K, Golan Y, Israelachvili J: The role of interparticle and external forces in nanoparticle assembly. *Nat Mater* 2008, **7**:527-538.
- Choi O, Deng KK, Kim N-J, Ross L, Surampalli RY, Hu Z: The inhibitory effects of silver nanoparticles, silver ions, and silver chloride colloids on microbial growth. *Water Res* 2008, **42**:3066-3074.
- Sperling RA, Parak WJ: Surface modification, functionalization and bioconjugation of colloidal inorganic nanoparticles. *Philos Trans R Soc A* 2010, **368**:1333-1383.
- Bartczak D, Kanaras AG: Diacetylene-Containing ligand as a new capping agent for the preparation of water-soluble colloidal nanoparticles of remarkable stability. *Langmuir* 2010, **26**:7072-7077.
- Karakoti AS, Das S, Thevuthasan S, Seal S: PEGylated inorganic nanoparticles. *Angew Chem Int Ed* 2011, **50**:1980-1994.
- Luo C, Zhang Y, Zeng X, Zeng Y, Wang Y: The role of poly(ethylene glycol) in the formation of silver nanoparticles. *J Colloid Interface Sci* 2005, **288**:444-448.
- Shkilnyy A, Soucé M, Dubois P, Warmont F, Saboungi M-L, Chourpa I: Poly(ethylene glycol)-stabilized silver nanoparticles for bioanalytical applications of SERS spectroscopy. *Analyst* 2009, **134**:1868-1872.
- Turkevich J, Stevenson PC, Hillier J: A study of the nucleation and growth processes in the synthesis of colloidal gold. *Discuss Faraday Soc* 1951, **11**:55-75.
- Bohren CF, Huffman DR: *Absorption and Scattering of Light by Small Particles* New York: John Wiley & Sons; 1998.

37. Aherne D, Ledwith DM, Gara M, Kelly JM: **Optical properties and growth aspects of silver nanoprisms produced by a highly reproducible and rapid synthesis at room temperature.** *Adv Funct Mater* 2008, **18**:2005-2016.
38. Li W, Guo Y, Zhang P: **SERS-active silver nanoparticles prepared by a simple and green method.** *J Phys Chem C* 2010, **114**:6413-6417.
39. Frens G: **Controlled nucleation for the regulation of the particle size in monodisperse gold suspensions.** *Nature (London), Phys Sci* 1973, **241**:20-22.
40. Toshima N, Yonezawa T: **Bimetallic nanoparticles—novel materials for chemical and physical applications.** *New J Chem* 1998, **22**:1179-1201.
41. Quinten M: *Optical Properties of Nanoparticle Systems: Mie and beyond* Weinheim: Wiley-VCH; 2011.
42. Wu D, Xu X, Liu X: **Electric field enhancement in bimetallic gold and silver nanoshells.** *Solid State Commun* 2008, **148**:163-167.
43. Bruzzone S, Arrighini GP, Guidotti C: **Theoretical study of the optical absorption behavior of Au/Ag core-shell nanoparticles.** *Mater Sci Eng C* 2003, **23**:965-970.
44. Chen HM, Liu RS, Jang L-Y, Lee J-F, Hu SF: **Characterization of core-shell type and alloy Ag/Au bimetallic clusters by using extended X-ray absorption fine structure spectroscopy.** *Chem Phys Lett* 2006, **421**:118-123.
45. Fahnestock KJ, Manesse M, McIlwee HA, Schauer CL, Boukherroub R, Szunerits S: **Selective detection of hexachromium ions by localized surface plasmon resonance measurements using gold nanoparticles/chitosan composite interfaces.** *Analyst* 2009, **134**:881-886.

doi:10.1186/1556-276X-7-151

Cite this article as: Stevenson *et al.*: Three strategies to stabilise nearly monodispersed silver nanoparticles in aqueous solution. *Nanoscale Research Letters* 2012 **7**:151.

Submit your manuscript to a SpringerOpen[®] journal and benefit from:

- Convenient online submission
- Rigorous peer review
- Immediate publication on acceptance
- Open access: articles freely available online
- High visibility within the field
- Retaining the copyright to your article

Submit your next manuscript at ► springeropen.com
